

Supplementary Information

Origin of adsorption trends in two-dimensional single-atom catalysts via d-state filling

Yuhao Qiu^{ab}, Weiqi Song^{ab}, Huimin Hu^{*ab}, and Jin-Ho Choi^{*ab}

^a College of Energy, Soochow Institute for Energy and Materials InnovationS,

Soochow University, Suzhou 215006, China

^b Key Laboratory of Advanced Carbon Materials and Wearable Energy Technologies

of Jiangsu Province, Soochow University, Suzhou 215006, China

Table S1 Adsorption energies of atomic intermediates (H, C, N, O, Si, P, and S) on transition-metal dopants in N-doped graphene.

Dopant	H (k = 1)	C (k = 2)	N (k = 3)	O (k = 4)	Si (k = 2)	P (k = 3)	S (k = 4)
Sc ($v_m = 3$)	-3.074	-3.469	-4.202	-5.592	-2.254	-2.398	-3.155
Ti ($v_m = 4$)	-3.248	-4.216	-6.187	-8.184	-2.745	-3.328	-4.999
V ($v_m = 5$)	-2.897	-4.824	-7.388	-8.028	-2.729	-3.725	-4.787
Cr ($v_m = 6$)	-2.487	-4.662	-6.959	-6.317	-2.588	-3.370	-3.247
Mn ($v_m = 7$)	-2.396	-5.309	-6.522	-5.197	-2.994	-3.017	-2.610
Fe ($v_m = 8$)	-2.535	-5.608	-5.164	-4.784	-3.497	-2.690	-2.722
Co ($v_m = 9$)	-2.599	-3.729	-3.918	-3.394	-2.624	-2.163	-1.823
Ni ($v_m = 10$)	-1.128	-1.735	-2.326	-1.932	-1.181	-0.736	-0.497
Y ($v_m = 3$)	-2.914	-2.564	-3.946	-5.081	-2.162	-2.230	-2.944
Zr ($v_m = 4$)	-3.658	-4.250	-5.927	-8.136	-2.936	-3.387	-5.109
Nb ($v_m = 5$)	-3.496	-5.204	-7.869	-8.732	-3.396	-4.402	-5.546
Mo ($v_m = 6$)	-3.054	-6.359	-8.727	-8.661	-3.961	-5.138	-5.496
Tc ($v_m = 7$)	-3.195	-6.983	-8.805	-7.610	-4.564	-5.214	-4.812
Ru ($v_m = 8$)	-3.280	-7.126	-6.867	-5.462	-4.900	-4.179	-3.557
Rh ($v_m = 9$)	-2.930	-4.251	-4.069	-3.427	-3.133	-2.502	-2.071
Pd ($v_m = 10$)	-0.830	-1.446	-1.876	-1.375	-1.179	-0.494	-0.364
Hf ($v_m = 4$)	-3.851	-4.344	-5.859	-8.148	-2.554	-3.549	-5.237
Ta ($v_m = 5$)	-3.786	-5.253	-7.837	-8.911	-3.582	-4.625	-5.893
W ($v_m = 6$)	-3.705	-6.547	-8.921	-9.083	-4.324	-5.513	-6.042
Re ($v_m = 7$)	-3.523	-7.287	-9.089	-8.308	-5.040	-5.732	-5.529
Os ($v_m = 8$)	-3.310	-7.359	-7.605	-5.963	-5.168	-4.718	-3.913
Ir ($v_m = 9$)	-3.008	-5.022	-4.320	-3.667	-3.544	-2.691	-2.275
Pt ($v_m = 10$)	-1.089	-2.136	-1.902	-1.636	-1.410	-0.671	-0.590

Table S2 Adsorption energies of atomic intermediates (H, C, N, O, Si, P, and S) on transition-metal dopants in WS₂.

Dopant	H (k = 1)	C (k = 2)	N (k = 3)	O (k = 4)	Si (k = 2)	P (k = 3)	S (k = 4)
Sc ($v_m = 3$)	-3.081	-3.820	-5.774	-7.772	-2.458	-2.982	-5.457
Ti ($v_m = 4$)	-3.143	-4.319	-7.064	-8.044	-2.690	-3.993	-5.621
V ($v_m = 5$)	-2.731	-4.838	-7.178	-7.609	-2.579	-3.594	-5.337
Cr ($v_m = 6$)	-2.803	-5.121	-6.777	-6.532	-2.796	-3.428	-4.480
Mn ($v_m = 7$)	-2.975	-5.820	-7.053	-5.984	-3.410	-3.666	-4.551
Fe ($v_m = 8$)	-2.676	-5.948	-6.276	-5.451	-3.786	-3.603	-4.274
Co ($v_m = 9$)	-2.362	-5.237	-5.261	-5.105	-3.708	-3.299	-3.962
Ni ($v_m = 10$)	-2.076	-3.516	-3.832	-3.945	-2.780	-2.125	-3.244
Y ($v_m = 3$)	-3.047	-3.707	-5.606	-7.614	-2.418	-2.895	-5.409
Zr ($v_m = 4$)	-3.338	-4.689	-7.254	-8.302	-2.856	-3.698	-5.925
Nb ($v_m = 5$)	-3.289	-5.431	-7.999	-8.472	-3.388	-4.352	-6.080
Mo ($v_m = 6$)	-2.970	-6.410	-8.275	-8.405	-3.905	-4.748	-6.081
Tc ($v_m = 7$)	-2.929	-6.808	-8.372	-7.491	-4.209	-4.841	-5.541
Ru ($v_m = 8$)	-2.624	-6.969	-7.171	-5.876	-4.635	-4.316	-4.696
Rh ($v_m = 9$)	-2.523	-5.734	-5.220	-4.574	-4.081	-3.403	-3.717
Pd ($v_m = 10$)	-1.923	-3.325	-3.456	-3.031	-2.808	-1.909	-2.750
Hf ($v_m = 4$)	-3.408	-4.377	-6.683	-8.106	-2.719	-3.642	-5.925
Ta ($v_m = 5$)	-3.606	-5.402	-7.770	-8.843	-3.494	-4.548	-6.635
W ($v_m = 6$)	-3.599	-6.536	-8.543	-8.981	-4.182	-5.273	-6.812
Re ($v_m = 7$)	-3.512	-6.951	-8.682	-8.358	-4.574	-5.485	-6.517
Os ($v_m = 8$)	-3.239	-7.260	-8.069	-7.230	-5.073	-5.261	-5.907
Ir ($v_m = 9$)	-3.038	-6.660	-6.911	-5.624	-4.942	-4.806	-4.854
Pt ($v_m = 10$)	-2.781	-5.430	-4.817	-4.250	-4.428	-3.411	-3.893

Table S3 Adsorption energies of molecular intermediates (CO, NO, H₂O, NH₃, N₂, and NNH) on 4d transition-metal dopants in N-doped graphene.

Dopant	CO	NO	H ₂ O	NH ₃	N ₂	NNH (linear)	NNH (bent)
	(k = 2)	(k = 3)	(k = 2)	(k = 2)	(k = 2)	(k = 3)	(k = 1)
Y (v _m = 3)	-0.971	-2.278	-0.924	-1.058	-0.745	-1.977	–
Zr (v _m = 4)	-1.451	-3.085	-1.026	-1.205	-1.107	-2.898	–
Nb (v _m = 5)	-1.886	-3.631	-0.677	-1.035	-1.185	-3.307	–
Mo (v _m = 6)	-2.167	-4.062	-0.739	-1.180	-1.308	-3.550	–
Tc (v _m = 7)	-2.507	-4.149	-0.523	-1.081	-1.177	-3.546	–
Ru (v _m = 8)	-2.742	-3.020	-0.335	-1.105	-1.352	–	-2.393
Rh (v _m = 9)	-0.830	-0.566	-0.319	-0.271	0.099	–	-1.661
Pd (v _m = 10)	-0.077	-0.100	-0.221	-0.139	-0.074	–	-0.222

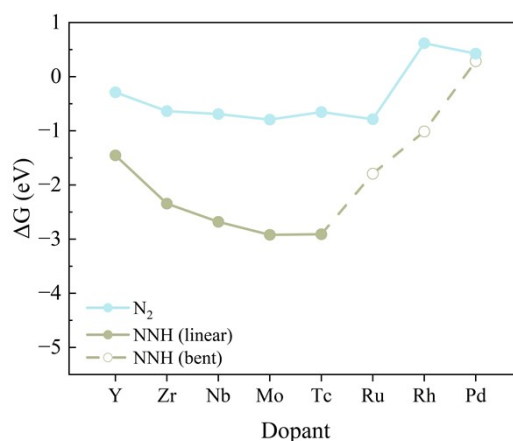


Fig. S1 Calculated Gibbs free energy (ΔG) of N₂ and NNH adsorption on the 4d dopant sites of N-doped graphene

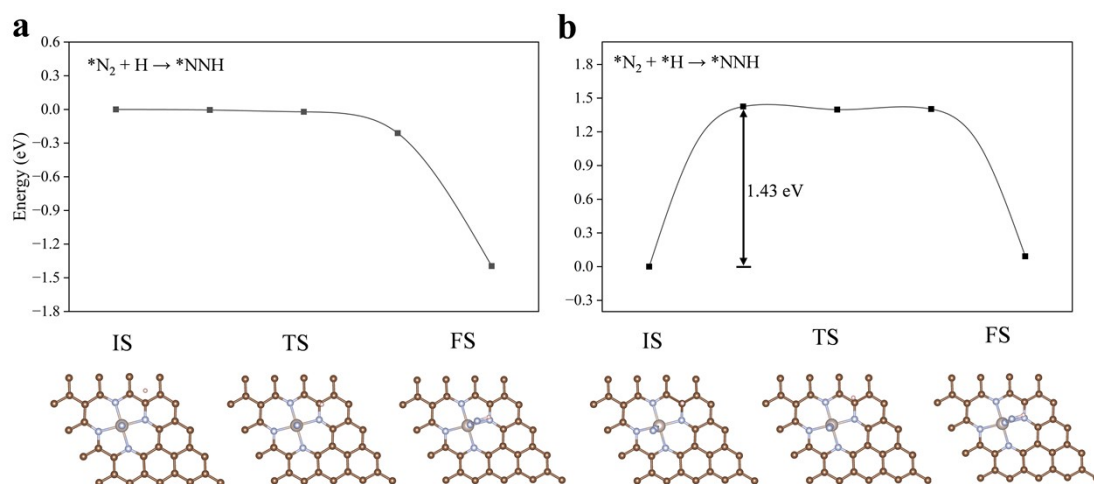


Fig. S2 Initial (IS), transition (TS), and final state (FS) configurations and the corresponding energy profiles for NNH formation. (a) Vacuum-assisted pathway, where N_2 reacts with a hydrogen species in the vacuum region; (b) Surface-mediated pathway involving an adsorbed hydrogen atom ($*H$) at the interfacial C-top site.

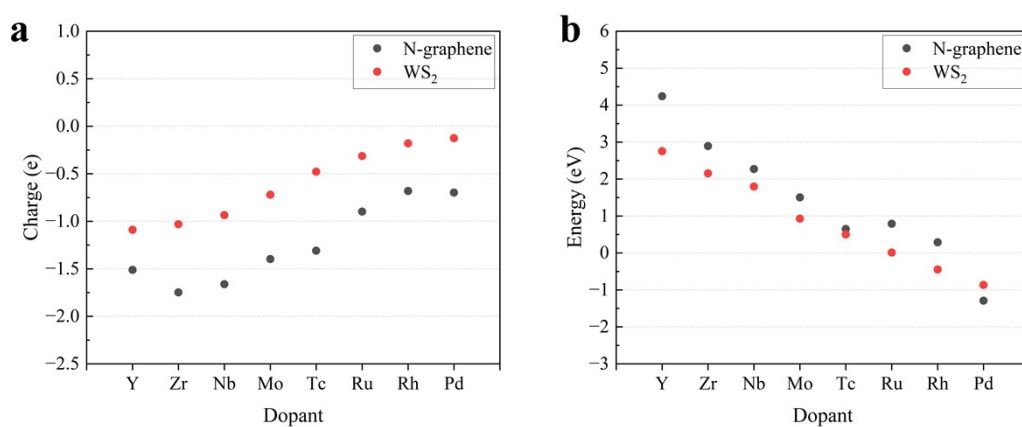


Fig. S3 (a) Comparison of Bader charges of 4d dopant metals on pristine N-doped graphene and WS_2 , where negative and positive values indicate electron loss and gain, respectively; (b) d-band center positions of the 4d dopant metals on WS_2 and N-doped graphene.

To ensure the numerical reliability of our calculations, we performed systematic convergence tests using N adsorption on 4d transition metals anchored on N-doped graphene as a representative model system. We compared our standard parameters (400 eV cutoff, $3\times 3\times 1$ k-point mesh) with more stringent settings (550 eV cutoff, $13\times 13\times 1$ k-point mesh). As shown in Fig. S4, the calculated adsorption energies exhibit a maximum deviation of only 0.055 eV across the entire 4d series, and more importantly, the qualitative trend—essential to the 10-electron rule—remains perfectly consistent. Furthermore, a comparison of the projected density of states (PDOS) for the d-orbitals of Tc shows that the electronic structures are virtually identical under both parameter sets. These results confirm that a 400 eV cutoff and the chosen k-point sampling provide a well-balanced compromise between computational efficiency and the required accuracy for describing both the energetic and electronic properties of these SAC systems.

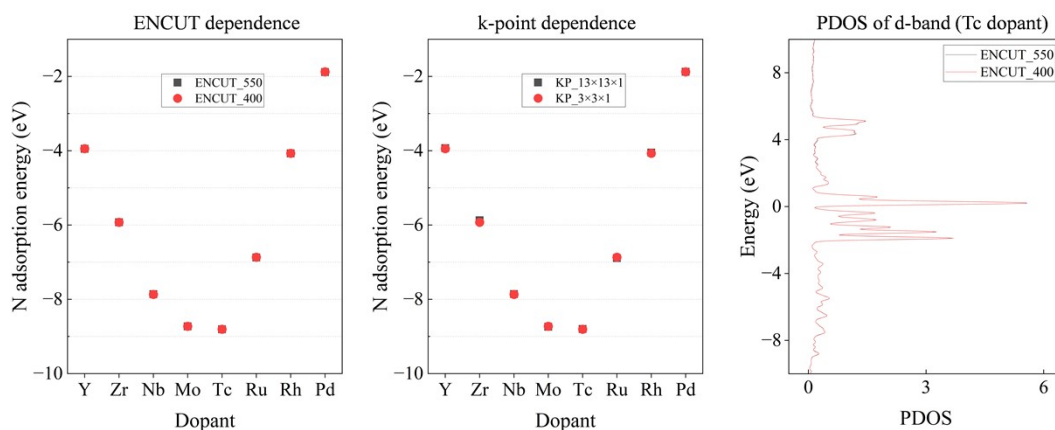


Fig. S4 Convergence tests for plane-wave cutoff energy and k-point sampling. Comparison of adsorption energies of N adatoms on N-doped graphene calculated with cutoff energies of 400 eV and 550 eV, and k-point meshes of $3\times 3\times 1$ and $13\times 13\times 1$. Also shown is the projected density of states (PDOS) of the d-band for the Tc dopant at different cutoff energies.

To verify that our conclusions are not sensitive to the choice of exchange–correlation

functional, we performed DFT+U calculations for N adsorption across the 4d series on N-doped graphene. The effective Hubbard parameters ($U_{\text{eff}} = U - J$) were adopted from the literature¹⁻⁴, with values for Y and Zr obtained by linear extrapolation:

$$U - J = 0.2131 \times n + 1.424$$

Where $n = 1$ for Y; $n = 2$ for Zr.

As shown in Fig. S5, the inclusion of U preserves the characteristic V-shaped adsorption energy trend across the series. Although a slight shift in the energetic minimum (from Tc to Mo) is observed, the overall trend remains unchanged. These results confirm that the 10-electron rule provides a robust qualitative framework, even when electron correlation effects are included.

Table S4 U-J parameters for DFT+U calculations¹.

Dopant	U / eV	J / eV	U-J / eV
Y	–	–	1.63
Zr	–	–	1.85
Nb	2.59	0.52	2.07
Mo	2.83	0.52	2.31
Tc	3.08	0.54	2.54
Ru	3.40	0.54	2.86
Rh	3.63	0.56	3.07
Pd	3.95	0.61	3.34

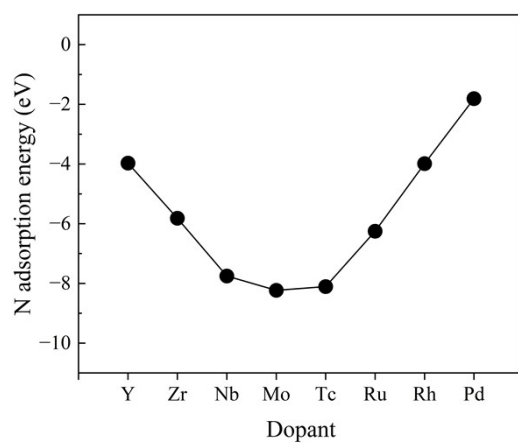


Fig. S5 N adsorption energies of 4d transition-metal dopants on N-doped graphene: DFT+U results.

References

- 1 I. V. Solovyev, P. H. Dederichs and V. I. Anisimov, *Phys. Rev. B*, 1994, **50**, 16861-16871.
- 2 G. Di Liberto, L. A. Cipriano and G. Pacchioni, *ACS Catal.*, 2022, **12**, 5846-5856.
- 3 H. Xu, D. Cheng, D. Cao and X. C. Zeng, *Nat. Catal.*, 2018, **1**, 339-348.
- 4 L. A. Cipriano, G. Di Liberto and G. Pacchioni, *ACS Catal.*, 2022, **12**, 11682-11691.